

# Dust-reddening and gravitational lensing of SDSS QSOs due to foreground damped Lyman- $\alpha$ systems

M. T. Murphy<sup>1</sup>\*, J. Liske<sup>2</sup>†

<sup>1</sup>*Institute of Astronomy, University of Cambridge, Madingley Road, Cambridge, CB3 0HA, UK*

<sup>2</sup>*European Southern Observatory, Karl-Schwarzschild-Str. 2, 85748 Garching, Germany*

Accepted —. Received —; in original form —

## ABSTRACT

We use Sloan Digital Sky Survey Data Release 2 QSO spectra to constrain the dust-reddening caused by intervening damped Ly $\alpha$  systems (DLAs). Comparing the spectral index distribution of a 79 sight-line DLA sample with that of a large control sample reveals no evidence for dust-reddening at  $z \sim 3$ . Our limit on the shift in spectral index,  $|\Delta\alpha| < 0.14$  ( $3\sigma$ ), corresponds to a limit on the colour excess due to SMC-like dust-reddening,  $E(B-V) < 0.01$  mag ( $3\sigma$ ). This is inconsistent with the early studies of Fall, Pei and collaborators who used the small, inhomogeneous QSO and DLA samples available. Comparison of the DLA and control magnitude distributions also reveals  $\approx 2\sigma$  evidence for an excess of bright and/or a deficit of faint QSOs with foreground DLAs. Higher equivalent width DLAs give a stronger signal. We interpret this as the signature of gravitational magnification due to the intervening DLAs.

**Key words:** dust, extinction – galaxies: high redshift – intergalactic medium – galaxies: ISM – quasars: absorption lines

## 1 INTRODUCTION

Dust, and its interaction with the gas phase, are key ingredients in any recipe for galaxy formation and evolution. Understanding the role of dust in the damped Lyman- $\alpha$  systems (DLAs) seen in QSO spectra is particularly important since DLAs are thought to comprise a significant fraction of the high redshift gas available for star-formation (e.g. Lanzetta et al. 1991). Information about dust in DLAs comes predominantly from the relative depletion of refractory (e.g. Fe) and non-refractory (e.g. Zn) elements onto dust grains (e.g. Pettini et al. 1997). This measures the amount of dust in DLAs but does little to constrain the dust’s composition or grain size.

DLA dust-reddening and extinction are potentially acute problems for flux-limited optical QSO surveys (e.g. Ostriker & Heisler 1984). Fall & Pei (1989) examined this by comparing the spectral indices of QSO spectra with and without foreground DLAs. They later detected (Fall, Pei & McMahon 1989) and confirmed (Pei, Fall & Bechtold 1991, hereafter PFB91) a significant difference between the spectral index distributions of the DLA and control samples, concluding that most DLAs will be missed by flux-limited surveys (Fall & Pei 1993). This is inconsistent with a recent radio-selected QSO survey for DLAs (Ellison et al. 2001) which finds that optical surveys underestimate the DLA number density per unit redshift by at most a factor of two.

The DLA and control samples of PFB91 are small (26 and 40 sight-lines respectively) and inhomogeneously selected, making it difficult to rule out large biases in colour and spectral index. The

Sloan Digital Sky Survey (SDSS; Stoughton et al. 2002) includes a large, homogeneous QSO sample with accurate spectrophotometric calibration and spectral resolution high enough ( $R \approx 1800$ ) to reliably detect DLAs (e.g. Prochaska & Herbert-Fort 2004). The SDSS therefore provides a powerful probe of DLA dust-reddening.

Another intriguing result is the recent  $\approx 4\sigma$  detection by Ménard & Péroux (2003) (hereafter MP03) of gravitational lensing (GL) caused by strong intervening Mg II absorbers in the 2dF QSO redshift survey. By comparing the magnitude distributions of the Mg II sample and a large control sample, they found an excess (deficit) of bright (faint) QSOs with absorbers and demonstrated that this was consistent with a GL interpretation. It is important to confirm and explore the GL produced by DLAs since, in principle, it provides a probe of the dark matter distribution in distant halos. Also, if the GL magnification of the DLA sample is large, DLA dust-reddened QSOs will be more detectable than those without, biasing any detection of dust-reddening.

In this paper, we select DLAs and, importantly, a large control sample of QSOs from the SDSS Data Release 2 (DR2; Abazajian et al. 2004) to constrain DLA dust-reddening (Section 3). We also independently confirm the GL effect and discuss the potential bias on reddening (Section 4). We present only the main observational results here, leaving most details to a later paper.

## 2 SELECTING DLAS FROM THE SDSS DR2

Spectra for all objects classified as QSOs in the SDSS DR2 with emission redshifts  $z_{\text{em}} > 2.4$  were visually inspected and the small

\* E-mail: mim@ast.cam.ac.uk (MTM); jliske@eso.org (JL)

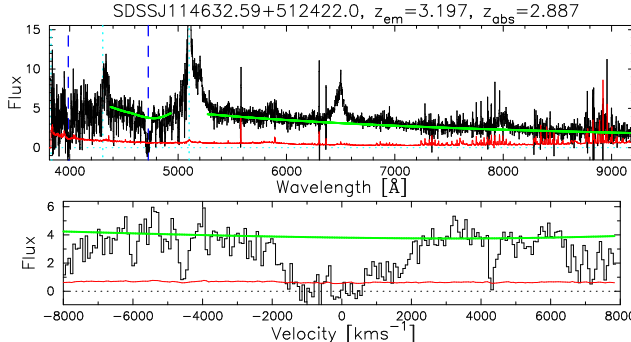


**Figure 1.** Top panel: Typical QSO with polynomial fit between the Ly $\beta$  and Ly $\alpha$  emission lines and power-law fit red-wards of Ly $\alpha$ . Dashed vertical lines mark the Ly $\alpha$  and Ly $\beta$  absorption lines. Bottom panel: Ly $\alpha$  absorption line. The lower solid line in both panels shows the SDSS 1  $\sigma$  error array.

number (< 1 per cent) which were clearly not QSOs at the SDSS-assigned emission redshift were rejected. We included those QSOs not listed as ‘primary’ targets in the SDSS, i.e. those which were not selected using the colour-space techniques of Richards et al. (2002). Other SDSS sources were selected from the FIRST and ROSAT surveys or could have been initially identified as stars or galaxies before spectroscopic follow-up. Our sample is therefore largely, though not strictly, homogeneously selected. The results are robust against this small inhomogeneity (Sections 3.2 & 4.2).

We search for DLAs between the Ly $\alpha$  and Ly $\beta$  emission lines and, to avoid DLAs intrinsic to the QSOs and moderately broad absorption lines (BALs), we ignore the regions  $< 10000$  km s $^{-1}$  below Ly $\alpha$  and above Ly $\beta$ . A continuum is formed by iteratively fitting a third-order polynomial to overlapping 20000-km s $^{-1}$  spectral chunks, rejecting pixels  $> 2\sigma$  below and  $> 5\sigma$  above the fit at each iteration until no more points are rejected ( $\sigma$  is the SDSS error array). The continuum chunks are combined by weighting each from zero at the edges to unity at the centre. Finally, the continuum is smoothed over 25 pixels ( $\sim 1700$  km s $^{-1}$ ). This procedure yields reliable continua in most cases. However, 3 likely DLAs were not selected due to poor fits near the continuum edges.

Candidate DLAs are identified as absorption features with rest-frame equivalent width  $W_r(\text{Ly}\alpha) \geq 10$  Å over a rest-frame  $\Delta\lambda_r = 15$  Å window. Close visual inspection of each DLA candidate is used to reject cases where no clear DLA profile is observed. This was the case for  $\sim 50\%$  of candidates and was more prominent at  $z_{\text{em}} > 3$  where the Ly $\alpha$  forest is thicker. Prochaska & Herbert-Fort (2004) advocate a DLA search strategy where no continuum is required and this may prove to be a more efficient future method. Nevertheless, our strategy will select the strongest DLAs which should be ideal for our study of dust-reddening and GL. Fig. 1 shows an example DLA.

We reject spectra where the signal-to-noise per pixel – (continuum) $_i$ /(1  $\sigma$  error) $_i$  for pixel  $i$  – drops below a threshold value of  $S/N_{\text{min}} = 2$  anywhere along the fitted continuum. Below this the algorithmic and visual assessment is unreliable. This is an important selection criteria for the GL study in Section 4 and we discuss it further there. We also reject QSOs with such severe BALs that DLA detection is unreliable, particularly those similar to LoBAL and FeLoBALs (e.g. Reichard et al. 2003). However, we kept QSOs with moderate BALs (e.g. HiBALs) since one can detect, and confidently not detect, DLAs in these cases. This is discussed further in Sections 3.2 & 4.2.

Fig. 2 shows the  $z_{\text{em}}$  and  $z_{\text{abs}}$  distributions for QSOs where a

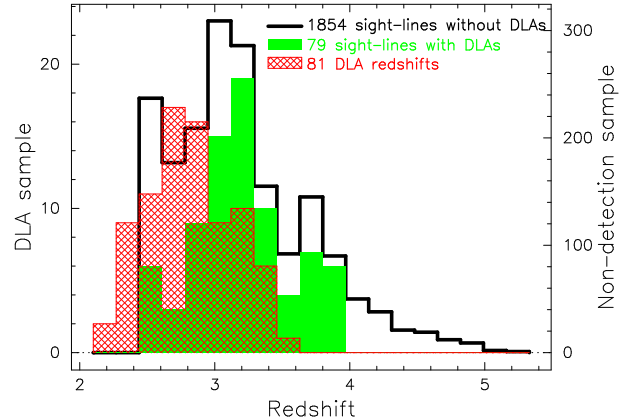


**Figure 2.**  $z_{\text{em}}$  distribution of QSOs with and without foreground DLAs (solid and hollow histograms). There are 1559 non-detections over the DLA sample’s  $z_{\text{em}}$  range. The hatched histogram shows the  $z_{\text{abs}}$  distribution.

DLA is and is not detected. We find 81 DLAs along 79 distinct QSO sight-lines. Although the DLA and non-detection  $z_{\text{em}}$  distributions are similar for  $2.4 < z_{\text{em}} < 4.0$ , there is a high- $z_{\text{em}}$  tail where no DLAs are detected. This is primarily because our DLA search is insensitive at high- $z_{\text{em}}$  where the Ly $\alpha$  forest is very thick.

### 3 DLA DUST-REDDENING

#### 3.1 Spectral index distributions

The spectral index,  $\alpha$ , defined as  $f_{\nu} \propto \nu^{\alpha}$ , was determined for each QSO by iteratively fitting a power-law to the flux  $> 10000$  km s $^{-1}$  red-wards of the Ly $\alpha$  emission line. Pixels  $> 4\sigma$  below or  $> 2\sigma$  above the fit were rejected at each iteration and iterations continued until no more points were rejected. An example fit is shown in Fig. 1. As well as avoiding intervening absorbers and the emission/absorption lines intrinsic to the QSO, this procedure effectively ignores the poorly sky-subtracted sections at  $\gtrsim 7000$  Å commonly found in SDSS spectra. The statistical errors in  $\alpha$  range from 0.01 to 0.35 with  $\gtrsim 80$  per cent of errors between 0.03 and 0.15.

Abazajian et al. (2004) discussed the DR2 spectrophotometric accuracy. There is a 0.03 mag dispersion in the difference between the  $r' - i'$  fibre colours and those derived by convolving the calibrated spectra with the filter transmission profiles. Thus, the error on the mean colour difference between a sample of 79 sight-lines and a large control sample is  $\approx 0.03/\sqrt{79} = 0.003$  mag. Hence, uncertainty in the spectrophotometry induces a mean spectral index difference of just  $|\Delta\alpha| \approx 0.01$  (Vanden Berk et al. 2001). Note also that we corrected the DR2 spectra for Galactic extinction using the Schlegel, Finkbeiner & Davis (1998)  $E(B-V)$  maps and the fitting formula of Pei (1992).

To form a representative control sample to which the DLA sample may be reliably compared, we drew 10000 bootstrap samples, each comprising 79 sight-lines, from the non-detection sample *with the same redshift distribution as the DLA sample*. There were 1559 non-detections over the  $z_{\text{em}}$  range of the DLA sample. Fig. 3 compares the  $\alpha$  distributions of the DLA and combined bootstrap sample. These are very similar to the ‘photometric spectral index’ distribution for SDSS QSOs derived by Richards et al. (2003). The error-bars on the DLA histogram represent the rms deviation in the number of non-detections in each bin over the 10000 bootstrap samples. To assess any differential reddening between the DLA and control samples, the number of DLA sight-lines per bin

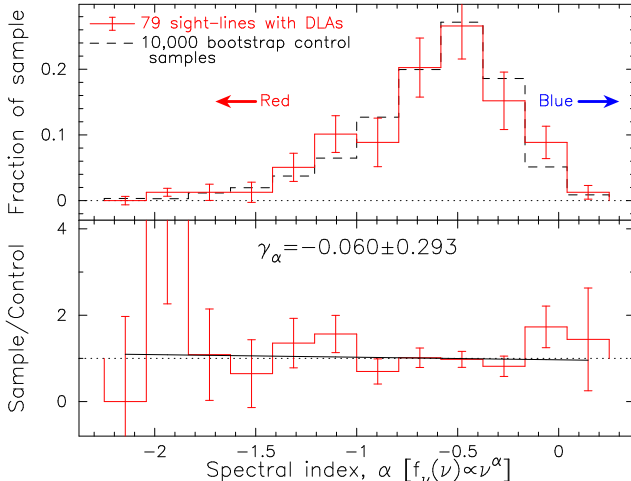


**Figure 3.** Top panel: Spectral index distributions of DLA and combined control samples. Error bars represent the rms over all bootstrap samples. Bottom panel: DLA-to-control number ratio with straight-line fit. The slope,  $\gamma_\alpha$ , is consistent with zero, i.e. no evidence for DLA dust-reddening.

is divided by the number in the combined control sample for that bin, normalized by the total sample sizes. This fraction is plotted in the lower panel of Fig. 3 and fitted by a straight line with slope  $\gamma_\alpha = -0.06 \pm 0.29$  which varies by  $< 0.3\sigma$  with different binning. The expected dispersion in  $\gamma_\alpha$  can be compared with the statistical error bar quoted here by treating each bootstrap sample in the same way as the DLA sample above, deriving a slope  $\gamma_{\text{boot}}$  for each. The distribution of  $\gamma_{\text{boot}}$  is well-fitted by a Gaussian, is centred on  $\gamma_{\text{boot}} = 0.0$  and has an rms of  $\sigma_{\text{boot}} = 0.31$ .

Fig. 3 shows no evidence for differential dust-reddening of SDSS DR2 QSOs due to foreground DLAs. By artificially altering the measured spectral indices for the DLA sample by different amounts we derive a  $1\sigma$  limit for  $\Delta\alpha$  allowed by the data,  $\Delta\alpha = -0.01 \pm 0.04$ . This is inconsistent with the claimed detection of dust-reddening by PFB91,  $\Delta\alpha = -0.38 \pm 0.13$ , which the SDSS data rule out at  $> 8\sigma$ . Assuming a Small Magellanic Cloud (SMC) extinction law for the DLAs and using the fitting formula of Pei (1992), our limit on  $\Delta\alpha$  corresponds to a  $1\sigma$  limit on  $E(B-V) < 0.004$ . Another method for detecting DLA dust-reddening is to analyse the  $r' - z'$  distributions with a similar technique to that above. Using the point spread function (PSF) magnitudes, we see no differential colour:  $\Delta(r' - z') = 0.012 \pm 0.019$ .

### 3.2 Robustness, potential biases and selection effects

To test the robustness of the above null result to possible biases and/or selection effects, the data were subjected to the following tests, the numerical results of which are summarized in Table 1.

**Test 1:  $S/N_{\min}$ .** The  $S/N_{\min}$  threshold is a free parameter in our DLA selection process. Fig. 4a shows the distribution of  $S/N_{\min}$  for the DLA and control samples analysed in a similar way to the spectral indices. There is clearly a deficiency of low-S/N DLA detections, possibly indicating an underestimated  $S/N_{\min}$  threshold. If dust-reddening is significant and some low-S/N DLAs are missed, the DLA sample may be biased against dust-reddened QSOs. Figs. 4b & c show the same analysis using increased  $S/N_{\min}$  thresholds where DLA selection is more reliable. In both cases, no significant deficiency of low-S/N DLAs is seen

**Table 1.** Slopes and bootstrap rms (in parentheses) for different sub-samples and systematic error checks.  $N$  is the number of QSOs with foreground DLAs. Tests 1a, b & c use  $S/N_{\min}$  thresholds of 2, 3 and 4 respectively. All other tests of  $\gamma_\alpha$  use  $S/N_{\min} = 2$  and those of  $\gamma_{r'}$ ,  $\gamma_{i'}$  &  $\gamma_{z'}$  use  $S/N_{\min} = 3$ . Tests 6a & b are for the low- and high- $z$  samples respectively and tests 7a & b are for the low- and high- $W_r$  samples respectively. See text for descriptions of other tests.

Test	$N$	$\gamma_\alpha$	$\gamma_{r'}$	$\gamma_{i'}$	$\gamma_{z'}$
1a	79	<b>-0.06(0.31)</b>	-0.60(0.18)	-0.55(0.17)	-0.58(0.17)
1b	68	-0.25(0.36)	<b>-0.41(0.20)</b>	<b>-0.35(0.20)</b>	<b>-0.42(0.20)</b>
1c	48	-0.02(0.46)	-0.60(0.26)	-0.51(0.26)	-0.56(0.26)
2	72/48	0.15(0.33)	-0.03(0.24)	0.04(0.30)	0.01(0.27)
3	75/64	-0.03(0.31)	-0.37(0.21)	-0.30(0.20)	-0.38(0.20)
4	76/65	-0.26(0.34)	-0.38(0.21)	-0.38(0.21)	-0.47(0.21)
5	31/28	-0.01(0.45)	-0.40(0.31)	-0.27(0.31)	-0.30(0.29)
6a	43/37	0.37(0.51)	-0.44(0.30)	-0.34(0.28)	-0.38(0.28)
6b	36/31	-0.49(0.43)	-0.27(0.29)	-0.26(0.28)	-0.36(0.29)
7a	44/39	-0.08(0.41)	-0.18(0.26)	-0.16(0.25)	-0.22(0.25)
7b	35/29	0.06(0.44)	-0.75(0.31)	-0.69(0.31)	-0.76(0.31)

and there is no substantial change in  $\gamma_\alpha$  (Table 1). Thus, the lack of DLA dust-reddening is robust against this potential selection bias.

**Test 2: GL.** In Section 4 we assess the magnification of QSOs due to foreground DLAs. If both the GL effect and DLA reddening are significant then reddened QSOs will be preferentially brightened above our  $S/N_{\min}$  threshold. We test this by artificially dimming the DLA sample with a representative value for the GL magnification from Section 4,  $A = 0.35$  mag:  $A$  is added to  $r'$ ,  $i'$  and  $z'$  and  $S/N_{\min}$  is reduced accordingly for each DLA sight-line. Table 1 shows only a marginal increase in  $\gamma_\alpha$  for this test.

**Test 3: Primary targets.** All SDSS QSOs were included in our sample, rather than just those targeted by SDSS as QSOs based on their photometric colours. This represents a slight inhomogeneity in our sample selection. We have tested this by removing all ‘secondary’ QSO targets from the sample and repeating the analysis. The lack of DLA reddening is robust to this test (Table 1).

**Test 4: BALs.** Only the most severe BAL QSOs were removed from the sample in Section 2 since DLAs could still be easily detected towards moderate BAL QSOs. However, it is possible (though improbable) that heavily saturated Fe III  $\lambda 1122$  BALs may mimic DLAs. Also, it is well known that even moderate BALs are substantially redder than ‘normal’ QSOs (e.g. Reichard et al. 2003). To test these possibilities we removed those QSOs which, by visual inspection, have some BAL features, particularly near the C IV emission line. Once again, Table 1 shows robust results.

**Test 5: DR1.** Schneider et al. (2003) formed a homogeneous QSO catalogue from the SDSS DR1 (Abazajian et al. 2003). We applied our analysis to this DR1 QSO sample using the DR2 spectra since Abazajian et al. (2004) note the spectrophotometry of the DR2 is much improved. Although the DLA sample is small, we find consistent results using the Schneider et al. selection (Table 1).

**Test 6:  $z_{\text{em}}$ -split.** The rest-frame composite SDSS QSO spectrum of Vanden Berk et al. (2001) shows an increased continuum level between 2200 Å and 4000 Å due to many Fe II emission lines. Since the SDSS spectra cover observed wavelengths up to 9800 Å our fitting method will recover systematically redder spectral indices for QSOs with  $z_{\text{em}} \lesssim 3.2$ . However, there should be no differential shift between DLA and control sample. Nevertheless, as a general consistency test, we split the sample into low- $z$  ( $z_{\text{em}} \leq 3.2$ ) and high- $z$  portions. Table 1 shows the DLA sample to be somewhat bluer (redder) than the control sample for the low- $z$  (high- $z$ )

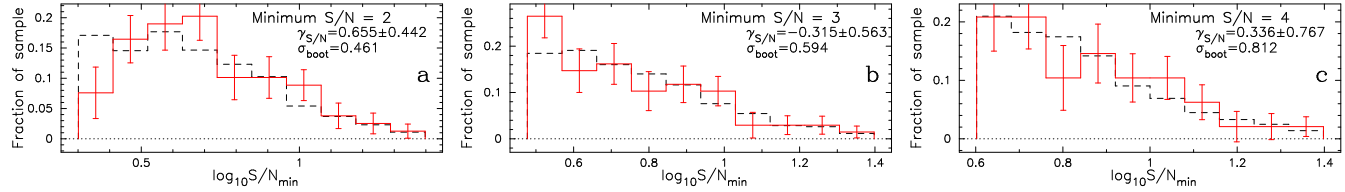


**Figure 4.** S/N distributions for the DLA (solid histogram) and combined control (dashed histogram) samples for different  $S/N_{\min}$  thresholds. Error bars are determined as in Fig. 3. With  $S/N_{\min} = 2$  we may miss some low-S/N DLAs but at higher  $S/N_{\min}$  the DLA selection is more reliable.

portions. Though this shift is only marginally significant, we note it here so that it can be tested with larger data-sets in future work.

**Test 7:  $W_r$ -split.** The rest equivalent width of the DLA line should be a measure of the H I column density,  $N(\text{H I})$ .  $W_r(\text{Ly}\alpha)$  was determined over a rest-frame  $\Delta\lambda_r = 15 \text{ \AA}$  window and so, for heavily damped systems, some absorption may be missed. Continuum errors and Ly $\alpha$  forest blending also contribute significantly to errors in  $W_r(\text{Ly}\alpha)$ . Nevertheless, if high- $N(\text{H I})$  DLAs cause more dust-reddening, splitting the sample into low- and high- $W_r$  ( $> 12.5 \text{ \AA}$ ) sub-samples may reveal this. However, Table 1 shows no difference in the  $\alpha$ -distributions for these sub-samples.

## 4 DLA GRAVITATIONAL LENSING

### 4.1 Magnitude distributions

Following the analysis of MP03, Fig. 5 compares the DLA and control PSF magnitude distributions. A  $S/N_{\min}$  threshold of 3 per pixel is used to ensure reliable DLA detection (Fig. 4), so the DLA sample comprises 68 sight-lines. The PSF magnitudes are corrected for Galactic extinction. Fig. 5 shows an excess of bright and/or a deficit of faint QSOs with DLAs relative to the control sample. The best-fitting slopes,  $\gamma_j$ , to the DLA/control ratio and the rms of  $\gamma_j$  for the bootstrap samples are given in Table 1 (test 1b) for each band  $j = r', i'$  and  $z'$ . The statistical significance of the differential brightening and/or dimming in each band is  $\approx 2\sigma$ .

Is the effect in Fig. 5 the signature expected from GL? MP03 note two main competing effects: (i) the flux density from the QSO is increased by the magnification factor  $\mu$ , and (ii) the solid angle in which lensed QSOs appear is increased, reducing the probability of observing them. MP03 show that a relative excess or deficit of lensed QSOs is expected depending on  $\mu$  and the gradient,  $\beta$ , of the control sample source counts as a function of magnitude,  $m$ :  $n(m)/n_0(m) \propto \mu^{2.5\beta(m)-1}$ , where  $n/n_0$  is the number ratio of lensed to unlensed QSOs and  $\beta(m) \equiv d \log_{10}[n_0(m)]/dm$ . Fig. 6 shows  $2.5\beta(m) - 1$  for the  $r'$ ,  $i'$  and  $z'$  bands: given the control samples in Fig. 5, GL should produce a relative excess of lensed QSOs for  $m \lesssim 19$  and a relative deficit for  $m \gtrsim 19$  in all bands. Note that the SDSS magnitude limit for  $z_{\text{em}} < 3$  QSOs is  $i' = 19.1$  whereas that for  $z_{\text{em}} > 3$  is  $i' = 20.2$  (Richards et al. 2002). Effectively, this implies that the derived faint-end slopes in Fig. 6 are too negative. However, using only  $z_{\text{em}} > 3$  QSOs we see no appreciable change in Fig. 6. The results in Fig. 5 are therefore *qualitatively* consistent with a GL interpretation. As in MP03, a simple illustrative example demonstrates plausible *quantitative* agreement: consider a DLA at an impact parameter of 10 kpc from a lens with an isothermal matter distribution and velocity dispersion  $\sigma_v = 200 \text{ km s}^{-1}$ . For  $z_{\text{em}} = 3.3$ ,  $z_{\text{abs}} = 2.8$ ,  $\Omega_m = 0.3$ ,  $\Omega_\Lambda = 0.7$  and  $H_0 = 70 \text{ km s}^{-1} \text{ Mpc}^{-1}$ , the magnification factor is  $\mu \approx 1.06$ . Fig. 6 therefore implies expected gradients  $\gamma_j \approx -0.15$  in Fig. 5.

### 4.2 Robustness and potential systematic effects

Despite the above result's low statistical significance ( $\approx 2\sigma$ ), it is surprisingly robust:  $\gamma_j$  varies by  $\lesssim 1\sigma$  over all the relevant tests in Table 1. Test 1 ( $S/N_{\min}$ ) is particularly important since, by placing the  $S/N_{\min}$  threshold too low, DLAs towards fainter QSOs may be preferentially missed and the effect observed in Fig. 5 may be artificially produced. Indeed, with a  $S/N_{\min}$  threshold of 2 per pixel, where Fig. 4a shows a deficit of low-S/N DLA-bearing sight-lines, Table 1 shows more negative slopes,  $\gamma_j$ . However, we see similar results even with a more conservative threshold of 4 per pixel where DLA detection is much more reliable.

Some possible alternative explanations for the effect in Fig. 5 are explored by MP03. One of the strongest potential systematic errors identified was dust obscuration by the DLAs, leading to a relative excess of faint QSOs in the DLA sample. In Section 3 we obtained a  $1\sigma$  limit on the colour excess induced by SMC-like dust in the DLAs,  $E(B-V) < 0.004 \text{ mag}$ . This corresponds to a total extinction of just  $Av \approx 0.01 \text{ mag}$  in the rest-frame  $V$ -band of the DLAs. Therefore, the GL magnification completely dominates the dust obscuration in the SDSS DLA sample.

## 5 DISCUSSION AND CONCLUSIONS

The SDSS provides a homogeneous QSO database which is ideal for studying DLA properties with respect to large, carefully selected control samples. We have utilised the SDSS DR2 to search for two important effects DLAs may have on background QSO light, dust-reddening and gravitational lensing (GL).

We find no evidence for dust-reddening of QSOs by foreground DLAs. The 79 sight-line DLA sample has a spectral index distribution consistent with that of our combined control sample (Fig. 3), ruling out overall shifts of  $|\Delta\alpha| > 0.14$  at  $3\sigma$ . This corresponds to a limit on the colour excess due to SMC-like dust of  $E(B-V) < 0.01 \text{ mag}$  ( $3\sigma$ ). Note that this is broadly consistent with the reddening expected from the level of Fe depletion with respect to Zn found in most DLAs. For a typical DLA with metallicity  $[\text{Zn}/\text{H}] = -1.5$  and dust-depletion factor  $[\text{Fe}/\text{Zn}] = -0.3$ , the dust-to-gas ratio is  $\kappa \approx 0.02$  times that found in the local ISM. For  $N(\text{H I}) = 10^{21} \text{ cm}^{-2}$ , this implies a shift in  $\alpha$  of just  $\Delta\alpha \approx -0.06$  (PFB91) or  $E(B-V) \approx 0.005 \text{ mag}$  for a SMC extinction law. The concept of a 'typical'  $\kappa$  for DLAs is, however, a poor one since  $[\text{Zn}/\text{H}]$  and  $[\text{Fe}/\text{Zn}]$  vary from DLA to DLA by more than 1.5 and 0.8 dex respectively. For example,  $\kappa \gtrsim 0.1$  is found for DLAs containing H<sub>2</sub> (Ledoux et al. 2003). Nevertheless, future comparison of dust-reddening and depletion in a large sample of DLAs may lead to constraints on the dust's grain size and/or composition.

The SDSS is a colour-selected QSO survey and so is biased against intrinsically very red and heavily dust-reddened spectra. Therefore, our results do not rule out a population of extremely dust-reddened QSOs (e.g. Gregg et al. 2002). Applying a SMC ex-

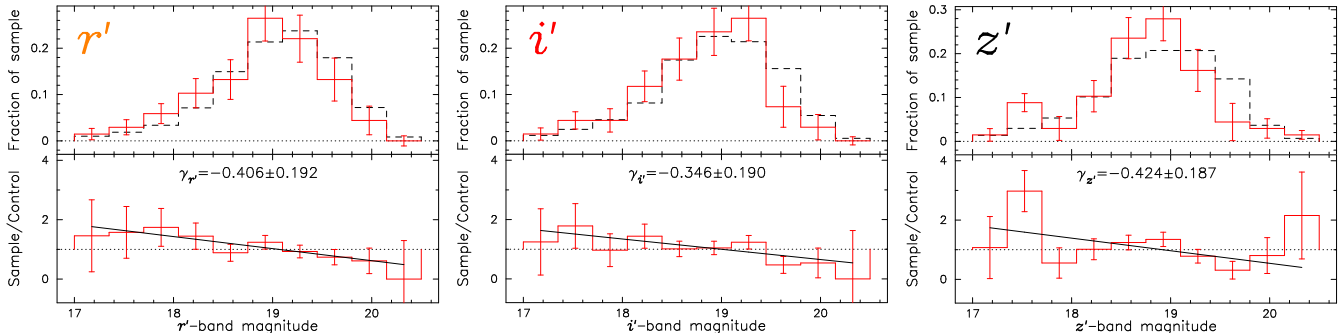


**Figure 5.** Top panels: PSF magnitude distributions for the DLA (solid histogram) and combined control (dashed histogram) samples. Error bars are determined as in Fig. 3. Bottom panels: DLA-to-control ratio with straight-line fit. The slopes,  $\gamma_j$ , indicate an excess of bright and/or a deficit of faint QSOs with DLAs.

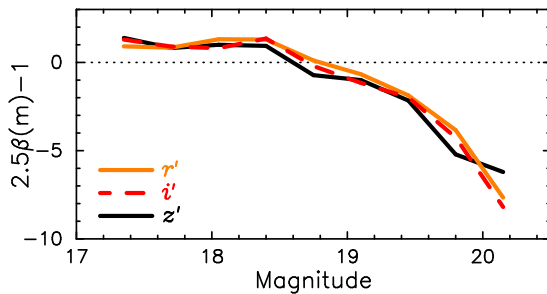


**Figure 6.**  $2.5\beta(m) - 1$  as a function of  $r'$ ,  $i'$  and  $z'$  PSF magnitude. GL will cause an excess (deficit) of bright (faint) QSOs with foreground DLAs.

tinction law with  $E(B-V) = 0.1$  mag (i.e.  $\Delta\alpha \approx -1.2$ ) to simulated QSO spectra, Richards et al. (2003) find the SDSS QSO survey completeness to be largely unchanged. That is, the  $\alpha$  distributions in Fig. 3 are sensitive to  $\Delta\alpha \gtrsim -1.0$  without large biases due to colour-selection. Richards et al. also find that only 6 per cent of QSOs have spectra consistent with SMC-like dust-reddening with  $E(B-V) > 0.04$  mag and they interpret the reddening to be internal to the QSO host-galaxy. This is consistent with our results.

However, our results are inconsistent with the those of PFB91 who found a mean  $\Delta\alpha = -0.38 \pm 0.13$ . The metallicities and dust-depletion factors for the DLAs used by PFB91 are not especially different to those of the overall DLA population. We suggest that a combination of small-number statistics and sample inhomogeneity may have affected their results. Two notable differences between the SDSS and PFB91 QSO samples are that the SDSS contains much fainter QSOs and extends to slightly higher  $z_{\text{em}}$  and  $z_{\text{abs}}$ . A huge increase in  $\kappa$  between the typical  $z_{\text{abs}}$  for the two samples,  $z_{\text{abs}} \approx 2.8$  and  $z_{\text{abs}} \approx 2.4$ , may therefore explain the discrepancy. However, this is unlikely given the results of various abundance studies (e.g. Prochaska et al. 2003; Curran et al. 2004).

We have also identified a possible signature of gravitational magnification of QSOs by foreground DLAs in a similar vein as MP03. We expect an excess of bright QSOs with DLAs and a deficit of faint QSOs with DLAs relative to our control sample, where the dividing line should fall at  $\sim 19$ th magnitude in  $r'$ ,  $i'$  and  $z'$ . This is indeed what is observed (Fig. 5). The amplitude of gravitational magnification, measured from the slope of the DLA/control ratio versus magnitude, also broadly agrees with that expected in a simple model of the QSO-DLA lensing system. The putative lensing signal, though significant only at  $\approx 2\sigma$ , is robust against a variety of systematic error and bias checks. Furthermore, a higher equivalent width sub-sample of DLAs gives a stronger signal, as would be expected if these DLAs had lower impact parameters. Refining

the above results with future SDSS samples is clearly important for future constraints on the dark matter halos of DLA host-galaxies.

## ACKNOWLEDGMENTS

We thank Bob Carswell, Paul Hewett and Max Pettini for discussions. MTM thanks PPARC for support at the IoA. Funding for the creation and distribution of the SDSS Archive has been provided by the Alfred P. Sloan Foundation, the Participating Institutions, the National Aeronautics and Space Administration, the National Science Foundation, the U.S. Department of Energy, the Japanese Monbukagakusho, and the Max Planck Society.

## REFERENCES

- Abazajian K. et al., 2003, AJ, 126, 2081
- Abazajian K. et al., 2004, AJ, submitted, preprint (astro-ph/0403325)
- Curran S. J., Webb J. K., Murphy M. T., Carswell R. F., 2004, MNRAS, accepted, preprint (astro-ph/0311357)
- Ellison S. L., Yan L., Hook I. M., Pettini M., Wall J. V., Shaver P., 2001, A&A, 379, 393
- Fall S. M., Pei Y. C., 1989, ApJ, 337, 7
- Fall S. M., Pei Y. C., 1993, ApJ, 402, 479
- Fall S. M., Pei Y. C., McMahon R. G., 1989, ApJ, 341, L5
- Gregg M. D., Lacy M., White R. L., Glikman E., Helfand D., Becker R. H., Brotherton M. S., 2002, ApJ, 564, 133
- Lanzetta K. M., McMahon R. G., Wolfe A. M., Turnshek D. A., Hazard C., Lu L., 1991, ApJS, 77, 1
- Ledoux C., Petitjean P., Srianand R., 2003, MNRAS, 346, 209
- Ménard B., Péroux C., 2003, A&A, 410, 33
- Ostriker J. P., Heisler J., 1984, ApJ, 278, 1
- Pei Y. C., 1992, ApJ, 395, 130
- Pei Y. C., Fall S. M., Bechtold J., 1991, ApJ, 378, 6
- Pettini M., King D. L., Smith L. J., Hunstead R. W., 1997, ApJ, 478, 536
- Prochaska J. X., Gawiser E., Wolfe A. M., Castro S., Djorgovski S. G., 2003, ApJ, 595, L9
- Prochaska J. X., Herbert-Fort S., 2004, PASP, accepted, preprint (astro-ph/0403391)
- Reichard T. A. et al., 2003, AJ, 125, 1711
- Richards G. T. et al., 2002, AJ, 123, 2945
- Richards G. T. et al., 2003, AJ, 126, 1131
- Schlegel D. J., Finkbeiner D. P., Davis M., 1998, ApJ, 500, 525
- Schneider D. P. et al., 2003, AJ, 126, 2579
- Stoughton C. et al., 2002, AJ, 123, 485
- Vanden Berk D. E. et al., 2001, AJ, 122, 549